ORIGINAL ARTICLE

CrossMark

Characterization of methanthelinium binding and function at human M_1–M_5 muscarinic acetylcholine receptors

Matthias Irmen[1] · Janine Holze[1] · Theresa Bödefeld[1] · Christian Tränkle[1]

Abstract

Firstly, it was determined whether methanthelinium bromide (MB) binds to human M_1–M_5 (hM_1–hM_5) muscarinic acetylcholine receptors in comparison to the classical muscarinic antagonist N-methylscopolamine (NMS). [^{3}H]NMS dissociation binding experiments revealed an allosteric retardation of dissociation at 100 μM of MB ranging from none in hM_3 to 4.6-fold in hM_2 receptors. Accordingly, global non-linear regression analysis of equilibrium inhibition binding curves between [^{3}H]NMS (0.2 and 2.0 nM) and MB was applied and compared using either an allosteric or a competitive model. The allosteric cooperativity of MB binding within MB/NMS/hM receptor complexes was strongly negative and undistinguishable from a competitive interaction throughout all subtypes. Applying the competitive model to the equilibrium binding data of MB and NMS, suggested competition at all hM subtypes: $\log K_I$ (± S.E.) $hM_3 = 8.71 \pm 0.15$, $hM_1 = 8.68 \pm 0.14$, $hM_5 = 8.58 \pm 0.07$, $hM_2 = 8.27 \pm 0.07$ to $hM_4 = 8.25 \pm 0.11$. Secondly, the effects of MB on acetylcholine (ACh) induced hM receptor function showed very strong negative allosteric cooperativity at all subtypes pointing against an allosteric antagonism of MB with ACh. Competition with ACh was characterized by $\log K_B$: $hM_1 = 9.53 \pm 0.05$, $hM_4 = 9.33 \pm 0.05$, $hM_5 = 8.80 \pm 0.05$, $hM_2 = 8.79 \pm 0.06$, to $hM_3 = 8.43 \pm 0.04$. In conclusion, MB, below 1 μM, binds competitively and non-selectively (except for the difference between hM_3 vs. hM_4) to all five hM receptor subtypes with nanomolar affinity and is able to *functionally inhibit* ACh responses in a competitive fashion, with a slight subtype preference for hM_1 and hM_4.

Keywords Allosteric · Hyperhidrosis axillaris · Muscarinic receptor · Methanthelinium bromide · NMS · Orthosteric

Abbreviations

ACh	acetylcholine
AChE	acetylcholinesterase
CHO-cells	Chinese hamster ovary cells
GDP	guanosine diphosphate
GPCR	G-protein coupled receptors
GTP	guanosine-5′-triphosphate
hM	human muscarinic receptor
IP$_1$	inositol monophosphate
MB	methanthelinium bromide
M$_1$	muscarinic acetylcholine receptor subtype 1
M$_2$	muscarinic acetylcholine receptor subtype 2
M$_3$	muscarinic acetylcholine receptor subtype 3
M$_4$	muscarinic acetylcholine receptor subtype 4
M$_5$	muscarinic acetylcholine receptor subtype 5
NMS	(−)-scopolamine methylbromide
PEI	polyethylenimin

✉ Christian Tränkle
traenkle@uni-bonn.de

[1] Pharmacology and Toxicology, Institute of Pharmacy, University of Bonn, Gerhard-Domagk-Straße 3, 53121 Bonn, Germany

Introduction

Muscarinic acetylcholine receptors possess a central role in the regulation of the human organism considering the huge amount of different physiological functions, such as smooth muscle contraction, regulation of heart rate, and glandular secretion (Wess 2004, Wess et al. 2007). They belong, like rhodopsin, to the class of G-protein-coupled-receptors (GPCR) and are attributed to the α-branch of class A GPCRs (Fredriksson et al. 2003). These GPCRs are a receptor protein superfamily consisting of about 800 different gene families (Lagerström and Schiöth 2008). The present study

focuses on the five *h*uman muscarinic acetylcholine receptors hM_1–hM_5 known until to date. Each of these subtypes displays a distinct pattern of distribution and can be distinguished by their preferred pathway of G-protein coupling. Two of these receptor subtypes, i.e., M_2 and M_4, have been demonstrated to couple to G-proteins of the $G_{i/o}$ family, whereas M_1, M_3, and M_5 receptors via their intracellular binding surface preferably bind to $G_{q/11}$ proteins (Caulfield and Birdsall 1998; Hulme et al. 1990). The M-receptors consist of one protein strand that passes the plasma membrane via seven transmembrane (TM) helices, which are connected by three intra- and three extracellular loops and are orientated in a circular manner to form a binding pocket (Kruse et al. 2014a, b).

The extracellular, orthosteric binding site (*ortho*; Greek for "right") for the endogenous neurotransmitter acetylcholine and for conventional orthosteric antagonists, such as the radioligand [3H]NMS applied in the current study, is situated within the upper third of the binding pocket and is highly conserved among the subtypes (Haga et al. 2012). In contrast, an allosteric (*allo*, Greek for "different") vestibule, which does not bind acetylcholine, is located in a more extracellular location within the area of the extracellular loops. This topology enables allosteric and orthosteric ligands to bind simultaneously to the receptor and to change their binding affinity in the resulting ternary alloster/orthoster/receptor-complex reciprocally. Depending on the change in equilibrium binding by an allosteric or orthosteric ligand, the behavior is termed either positive-, negative-, or neutral-cooperativity if both types of ligands promote, inhibit, or leave their affinity unchanged within the ternary complex with the receptor (Ehlert 1988). Moreover, cooperativity can be found and quantified on different levels, i.e., on a binding and on a functional level. To analyze such data, one can apply the ternary complex model of allosteric interactions (i.e., Stockton et al. 1983; Ehlert 1988; Lazareno and Birdsall 1995). Functional cooperativity can be explored, e.g., by the method of Hall (2000) or according to Lazareno and Birdsall (1995).

Thereby, the binding and functional properties of methanthelinium bromide (MB) (Fig. 1), a drug widely used for the therapy of hyperhidrosis axillaris (Hexsel and Camozzato 2018) were scrutinized at hM_1–hM_5 receptors to the best of our knowledge for the first time in detail. The current study gives new insights in MB binding, function, and its receptor subtype selectivity.

Methods

[3H]NMS (specific activity 70 Ci/mmol) and [35S]-GTPγS (specific activity 1250 Ci/mol) were purchased from PerkinElmer Life and Analytical Sciences (Boston, MA). MB, i.e., diethyl-methyl-[2-(9H-xanthene-9-carbonyloxy)ethyl] azanium bromide, $C_{21}H_{26}BrNO_3$
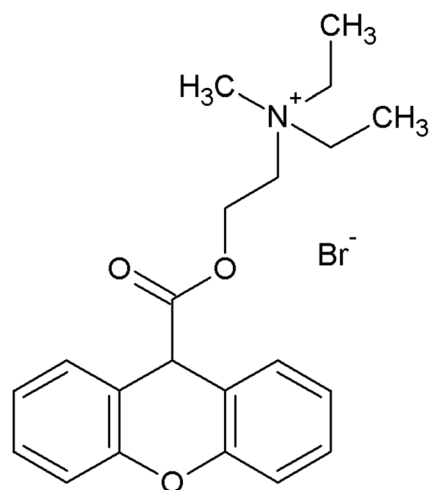

Fig. 1 Structural formula of methanthelinium bromide

(Vagantin™, Riemser Pharma), was synthesized by Laborchemie Apolda GmbH (Apolda, Germany). Atropine sulfate and $N(-)$-scopolamine methylbromide were obtained from Sigma Chemicals (München, Germany). All other laboratory reagents were obtained from Sigma-Aldrich unless otherwise specified.

Cell culture

Chinese hamster ovary cells (CHO-cells) stably transfected with the five human M-receptor genes were purchased from www.cdna.org, MO, USA to be applied in the current study. All cell lines were cultivated with 5% CO_2 at 37 °C in humidified atmosphere and all media were supplemented with 10% (*v/v*) FCS, penicillin (100 U ml^{-1}), and streptomycin (100 μg/ml). For equilibrium binding experiments with the radioligand [3H]NMS and [35S]GTPγS binding assays, cells were grown, harvested, homogenized, and processed as described elsewhere (Tränkle et al. 2003). The resulting membrane pellets were washed twice in 20-mM HEPES, 0.1-mM Na_4EDTA, pH 7.4, 4 °C ("storage buffer"), and the final pellets were stored as a membrane suspension in storage buffer at − 80 °C. Protein content was determined by the Lowry method and amounted to 1.5–3.5 mg ml^{-1}.

Radioligand-binding assay

The [3H]NMS filtration binding assay was carried out as described before (Schmitz et al. 2014). The incubation buffer was 10-mM HEPES, 10-mM $MgCl_2$, and 100-mM NaCl pH 7.4 at 30 °C (P1). Briefly, [3H]NMS equilibrium binding assays used 0.2- and 1.0-nM [3H]NMS and 10–40-μg protein/ml membranes. Non-specific [3H]NMS binding was determined in the presence of

1-μM atropine and did not exceed 5% of total binding. Equilibrium binding experiments were performed in 96-well microtiter deep well plates (Abgene House, Epsom, U.K.) in a final volume of 500 μl. The incubation time necessary to equilibrate [³H]NMS binding in the presence of an allosteric modulator was calculated according to the following equation (Lazareno and Birdsall 1995):

$$t_{0.5_{obs}} = t_{0.5_{off}} \times \left(1 + K_{X,diss} \cdot [X]\right) \qquad (1)$$

$t_{0.5_{obs}}$ is an estimate of [³H]NMS association half-life time in the presence of allosteric modulator X, $t_{0.5_{off}}$ is the half-life time of [³H]NMS dissociation in the absence of allosteric modulator, and $K_{X,diss}$ was taken as the affinity constant of the modulator at NMS occupied receptor, i.e., the inverse of the concentration at which the half-life time of [³H]NMS dissociation is doubled. Equilibrium was assumed to be reached after $5 \times t_{0.5_{obs}}$. Incubation times amounted to 2 h (hM1–hM4) or 4 h (hM5). Receptor bound radioactivity was separated by filtration on a Tomtech 96-well Mach III Harvester (Wallac®) using glass fiber filtermats (Filtermat A®, Wallac, Turku, Finland), which had been pretreated with 0.1% polyethyleneimine to reduce non-specific filter binding. Filtration was followed by two rapid washing steps (0.8 ml of 100-mM NaCl, 4 °C, 1.7 s). Filtermats were dried for 3 min at 400 W in a microwave oven. Thereafter, scintillation wax (Meltilex® A, Wallac, Turku, Finland) was melted for 1 min at 90 °C onto the filtermat using a Dri-Block® DB-2A (Techne, Duxford Cambridge, UK). The filters were placed in sample bags (Wallac, Turku, Finland), and filter bound radioactivity was measured using a Microbeta Trilux-1450 scintillation counter (Wallac, Turku, Finland).

Kinetic experiments

Radioligand association

For association experiments, membranes were preincubated with incubation buffer for 15 min at 30 °C before the radioligand was added at different time intervals applying a reverse time protocol (Williams 1993) over 60 (hM₂)–180 min (hM₅) followed by simultaneous filtration of all samples. Non-specific binding was determined in parallel throughout all experiments in the presence of 10-μM atropine.

Radioligand dissociation

For dissociation experiments, membranes were incubated with the radioligand for 60 min at 30 °C. Thereafter, aliquots of the mixture were added to an excess of

unlabelled ligand in buffer over a total period of 120 min followed by simultaneous filtration of all samples. To determine the effect of MB on the dissociation of [³H]NMS, dissociation was measured by addition of 10-μM atropine in combination with the test compound.

[³⁵S]GTPγS binding assay

[³⁵S]GTPγS binding assays were conducted as recently described (Bock et al. 2014). In brief, different amounts of membrane protein (20–40 μg ml⁻¹) of CHO-hM2 and CHO-hM4 cell homogenates were incubated with 0.07 nM of [³⁵S]GTPγS to measure the maximal agonist induced increase after 1 h of ACh stimulation alone or in combination with MB (see below) in the presence of 10 μM of GDP. All experiments were conducted in HEPES buffer. Bound [³⁵S]GTPγS was collected by filtration over glass fiber filters moistened with water.

Second messenger IP₁ accumulation in hM-CHO cells

Inositol monophosphate accumulation was measured as described before (Chen et al. 2014). The HTRF®-IP One kit (Cisbio International) was used for assessing IP₁ production in cells expressing hM₁, hM₃, and hM₅ receptors. In a 384-well format, the cell suspension was set to 50,000 (counted in a Neubauer chamber) cells per 7 μl per well. After 30 min of incubation at 37 °C and 5% CO₂, 7 μl of stimulation buffer was added containing either: (1) several concentrations of the endogenous agonist ACh alone (agonist control curve), or (2) a mixture of a fixed concentration of ACh and various concentrations of NMS or MB (inhibition curve), or (3) several concentrations of ACh in the presence of a fixed concentration of NMS or MB, respectively (antagonist shifted control curve). After further incubation at 37 °C and 5% CO₂ for 30 min, 3-μl IP₁-D2 conjugate followed by 3 μl of terbium cryptate-labeled anti-IP₁ antibody, diluted in lysis buffer, were added. After incubation at room temperature for another 60 min, time-resolved fluorescence was measured at 620 and 665 nm with a Mithras² LB 943 multimode reader (Berthold Technologies) according to the instructions of the manufacturer.

Data analysis

The binding and functional data from individual experiments were analyzed by computer-aided, non-linear regression analysis using Prism 5.03b (GraphPad Software®, San Diego, CA, USA). Presented are mean values ± standard errors throughout the manuscript. Unless otherwise indicated, concentration/effect curves were obtained by applying nonlinear regression analysis to data sets representing

individual curves using a four-parameter containing model-independent logistic equation:

$$Y = Bottom + \frac{(Top-Bottom)}{1 + 10^{((\log EC_{50} - \log X) \cdot n_H)}} \quad (2)$$

X is the drug concentration; Y is the response. The parameters "Top" and "Bottom" refer to the upper and lower plateaus of the sigmoidal curve, respectively. $\log EC_{50}$ denotes the $\log X$ at the inflection point of the sigmoidal curve, and n_H is the slope factor of the curve.

Binding experiments

Radioligand association—estimation of k_{+1}, k_{-1}, and $K_{L,kin}$

Curve fitting to the *association* data of specific [3H]NMS binding at two concentrations of radioligand (L1 = 0.2 and L2 = 1 nM) was based on monoexponential association function:

$$B_t = \left(\frac{[L]}{[L] + k_{-1}/k_{+1}} \right) \cdot B_{max} \cdot \left(1 - e^{-k_{+1} \cdot [L] + k_{-1} \cdot t} \right) \quad (3)$$

B_{max} maximum binding of L in Y units
L concentration of the radioligand [3H]NMS
k_{+1} rate constant of [3H]NMS association (1/M min)
k_{-1} rate constant of [3H]NMS dissociation (1/min)
$K_{L,kin}$ k_{+1}/k_{-1}, i.e., kinetically derived equilibrium association binding constant of [3H]NMS

Plotting t in Eq. (3) as the independent variable and B_t as the dependent variable, a global fit of the data with L1 and L2 as known constants yielded estimates for k_{+1}, k_{-1}, and B_{max}. $K_{L,kin}$, the kinetically derived equilibrium association binding constant of [3H]NMS, was calculated by the software as $K_{L,kin} = k_{+1}/k_{-1}$ and presented as a "transform to report" in the results sheet of the analyses.

Radioligand dissociation—estimation of k_{-1} and $K_{X,diss}$

[3H]NMS *dissociation* data were analyzed assuming a monoexponential decay as described before (Tränkle et al. 2003). In brief, the slowing actions of 100-μM MB on [3H]NMS dissociation were expressed as the % reduction of the apparent rate constant k_{-1} of [3H]NMS dissociation. Concentration-effect curves for the reduction of the [3H]NMS dissociation rate constant by MB were fitted to a three-parameter logistic function. The parameter "Top" was the value of k_{-1} measured in the absence of test compound and was fixed at 100%, whereas the "inflection point" was set as a

variable. The parameter "Bottom" was fixed at 0%. The resulting inflection point was taken to reflect the equilibrium association constant $K_{X,diss}$ at NMS occupied receptors and was applied in Eq. (1) to calculate the incubation time necessary to equilibrate the respective concentration of MB in the presence of [3H]NMS and the respective hM receptor subtype.

Homologous competition—determination of K_D and B_{max}

Homologous competition data obtained with [3H]NMS were analyzed using a four-parameter logistic function to yield estimates of the bottom and top plateaus, the inflection point (IC$_{50}$), and the slope factor, n, of the curve. If the observed slope factor did not differ significantly from unity (F test, $P >$ 0.05), the IC$_{50}$-values were estimated with n constrained to -1. The affinity constant (expressed as $\log K_L$) and B_{max} values for the radioligand were calculated according to DeBlasi et al. (1989). Note, that for the sake of simplicity, the tables within the "Results" section of the current study (cf. Tables 1–4 and S1–S4) list equilibrium affinity constants throughout ($K_{equilibrium \; association \; constant} = 1 / K_{equilibrium \; dissociation \; constant}$).

Heterologous competition–allosteric ternary complex model—determination of K_X and α

Firstly, analyses of the data for the effect of the test compounds on the specific binding of the orthosteric radioligand [3H]NMS were based on the allosteric ternary complex model (e.g., Ehlert 1988). We applied Eq. (2) from Lazareno and Birdsall (1995) in which B_{max} was replaced by Eq. (8) of the same study and in which a slope factor, n, was included (Tränkle et al. 2003):

$$B_{LX} = B_0 \cdot \frac{(1 + K_L \cdot [L]) \cdot (1 + \alpha \cdot (K_X \cdot [X])^n)}{1 + (K_X \cdot [X])^n + K_L \cdot [L] \cdot (1 + \alpha \cdot (K_X \cdot [X])^n)} \quad (4)$$

BL_X and B_0 denote the specific binding of the radioligand L ([3H]NMS) in the presence and absence of the cooperatively interacting agent X (in the current study: the test compound MB), respectively. Note that in Eq. (4), K_L and K_X are the equilibrium *affinity* constants for the binding of L and X, respectively, at the unliganded receptors; α is the cooperativity factor for the allosteric interaction between X and L. In the "Results" section the interaction of L (=NMS) with MB (=X) is given by $\alpha < 1$, $\alpha > 1$, and $\alpha = 1$, indicating negative, positive, and neutral cooperativity, respectively. The factor n represents the slope factor of the curve. If the observed slope factors did not differ significantly from unity (F test, $P >$ 0.05), n was constrained to 1. Plotting X as the independent variable and BL_X as the dependent variable, a global fit of the

data to Eq. 4 with L and K_L as known constants yielded estimates for K_X and α.

Heterologous competition–competition at one site—check for a competitive interaction of NMS with MB by K_i sharing in global analyses

To check for a competitive interplay between NMS and MB, the K_i value of the antagonist MB was determined directly as a shared parameter by global non-linear regression analysis to the equilibrium binding data obtained at 0.2- and 1-nM [³H]NMS using Eq. (5):

$$B_{LI} = nsb + \frac{B_0 - nsb}{1 + 10^{(\log[I] - \log K_i)} \cdot \dfrac{K_L}{K_L + [L]}} \qquad (5)$$

B_{LI}: radioligand binding in the presence of inhibitor, B_0: radioligand binding in the absence of inhibitor, nsb: nonspecific binding, I: the concentration of inhibitor, K_i: equilibrium inhibition constant of inhibitor, K_L: equilibrium dissociation constant of the radioligand, L: concentration of radioligand where L and K_L are the known concentration and equilibrium dissociation constant of the radioligand, respectively, which were treated as constants with B_{LI} as the dependent and I being the independent variable. Additionally, with each pair of curves, an alternative fit with non-shared K_i, i.e., individual values were performed; in no case this alternative fit yielded a significantly better fit compared to a fit with K_i being shared between the curves (F test, $P > 0.05$).

Heterologous competition—determination of K_i by single curve analysis

To finally determine the K_i values of the antagonist MB at hM_1–hM_5 receptor subtypes using the competitive binding single site model, non-linear regression analysis using Eq. (5) was applied to the inhibition binding data obtained at 0.2-nM [³H]NMS; this concentration allowed to characterize true MB binding constants at a low radioligand occupancy of 0.2 in the so called "zone A" of radioligand binding (Bennett and Yamamura 1985).

Functional experiments

Firstly, every single curve was analyzed model-independently using a four parameter logistic function (cf. Eq. 2) to check whether the Hill slope factor n_H was different from unity. Since this was not the case in any of the functional experiments conducted (F test, $P > 0.05$), n_H was set to unity during the analyses with the following Eqs. (6) and (7).

Determination of the cooperativity factor β and the allosteric equilibrium affinity constant K_X

To begin, we checked for an allosteric interaction between ACh and NMS or MB, respectively, by applying the following equation according to Tränkle et al. (2005):

$$Effect = \frac{(E_{max} - basal)}{\left(1 + \left\{ \dfrac{EC_{0.5,control}}{[A]} \times \dfrac{1 + [B] \cdot K_X}{1 + \beta \cdot [B] \cdot K_X} \right\}^n \right)} + basal \qquad (6)$$

K_X is the equilibrium affinity constant for the binding of B (i.e., MB is considered to be an allosteric agent here) at orthosterically unliganded hM receptors. The variable β represents the cooperativity factor for the interaction between ACh and MB in ternary complexes such as ACh/MB/hM receptor ($\beta > 1$, $\beta < 1$, $\beta = 1$ indicating positive, negative, and neutral cooperativity). It should be noted that if MB acted competitive, then the cooperativity was not different from $\beta = 0$ and Eq. (6) became the integrated Schild Eq. (7) (Lazareno and Birdsall 1995).

Determination of the Schild slope factor s and the equilibrium affinity constant K_B

In order to characterize the interaction between ACh and MB in functional experiments which showed any evidence for an allosteric action of MB, a modified Schild method (Arunlakshana and Schild 1959) was used (Waud 1975; Lazareno and Birdsall 1993; Tränkle et al. 2005). The fact that the logistic slope factor of the inhibition curve cannot be handled isolated from the agonist slope (Lazareno and Birdsall 1993), a simultaneous analysis of two data sets, meaning variable concentrations of ACh alone (control curve) and several titrations of MB (or NMS) in the presence of a fixed concentration of ACh which corresponds to 80–90% of its maximum effect (inhibition curve), was conducted. Additionally, a third concentration-effect curve for ACh, incubated with a fixed concentration of MB was accomplished to check a prerequisite for this approach, i.e., whether MB caused a parallel shift of the control curve with the same E_{max} and bottom plateau values at the different subtypes. The functional data obtained with MB and NMS were fitted to the following equation (Tränkle et al. 2005):

$$Effect = \frac{(E_{max} - basal)}{\left(1 + \left\{ \dfrac{EC_{0.5,control}}{[A]} \times (1 + [B]^s \cdot K_B) \right\}^n \right)} + basal \qquad (7)$$

$[A]$ is the concentration of the agonist, E_{max} and basal determine the maximum and minimum effects of ACh; n:

slope factor of the agonist curve (corresponding to the Hill slope factor), $EC_{0.5,control}$ is the concentration of agonist which is necessary to produce a half-maximal effect, $[B]$ is the concentration of the antagonist, K_B indicates the equilibrium affinity constant of B, and s the Schild slope factor. To differentiate between a competitive or a non-competitive interaction, we tested whether the Schild slope s set to unity in Eq. (7) yielded a statistically better fit to the data compared to a variable Schild slope s (F test). Throughout all subtypes this was not the case.

Statistics

Data are shown as means ± S.E.M. for n observations unless stated otherwise. Multiple comparisons were carried out using one-way ANOVA with Newman-Keuls post-test. Simple comparisons of experimental mean values were performed applying Student's t test; comparisons of means with individual fixed values were assessed by a one sample t test. The level of statistical significance was set to 95% ($P < 0.05$).

Results

Equilibrium binding and association binding kinetics of the radioligand [³H]NMS at M₁–M₅ receptors

To check for a correspondence of the K_L values obtained for [³H]NMS under equilibrium binding conditions (cf. Fig. S1 and Table S1) compared to non-equilibrium, i.e., kinetic, conditions, we performed association experiments (Fig. S2 and Table S2). [³H]NMS association to hM_1–hM_5 was measured at 0.2 and 1 nM, respectively, in order to estimate by simultaneous nonlinear regression analysis of the data the rate constant k_{+1} of [³H]NMS association, the rate constant k_{-1} of [³H]NMS dissociation and, finally, to calculate the kinetic affinity constant $K_{L,kin} = k_{+1}/k_{-1}$ (see "Methods"—"Data analysis" for details). The $K_{L,kin}$ values obtained at all five subtypes (Table S2) corresponded to the respective $K_{L,eq}$ of NMS with a deviation of less than 0.4 log units (Table S1). This finding suggested [³H]NMS binding to obey the law of mass action and the receptor occupation theory by Clark (1933) and thus validated the radioligand binding assay system with respect to equilibrium and kinetic binding (Motulsky and Christopoulos 2004; Hulme and Trevethick 2010) applied in the current study.

Effect of MB on the dissociation of the radioligand [³H]NMS from M₁–M₅ receptors

The action of MB on [³H]NMS dissociation is shown in Fig. 2. This experimental protocol allows to detect undoubtedly a potential allosteric effect on the kinetics of

an orthosteric ligand like [³H]NMS because the orthosteric site is blocked by the radioligand. [³H]NMS dissociation was studied in the absence and presence of 100-μM MB to check for any compound-induced allosteric change of the kinetics of the radioligand (Fig. 2a–e). MB delayed [³H]NMS dissociation compared to the control half-life (visualized by an excess of atropine, i.e., $1000–10,000 \times K_{L,atropine}$, added alone) between 1.3-fold in hM_3 receptors to 4.6-fold in hM_2 receptors, thereby indicating formation of ternary complexes (consisting of MB/NMS/hM-receptor subtype, respectively) at very high concentrations of MB in each hM subtype except for hM_3 (Fig. 2, Table 1). In Fig. 2f, the corresponding rate constants k_{-1} of [³H]NMS dissociation are illustrated; in the presence of 100-μM MB, only at M₃ receptors the k_{-1} value did not differ significantly from the control k_{-1} which was set to 100% (t test, $P > 0.05$). At all remaining M receptor subtypes, the k_{-1} values differed significantly from the control value (t test, $P < 0.05$) and indicated an allosteric action at this high concentration of MB.

Comparison of fits to equilibrium binding data of MB at hM_2 and hM_3 receptors: allosteric ternary complex model versus competition at a single site

In view of the above-mentioned results, we carried out heterologous inhibition experiments applying two concentrations of [³H]NMS (0.2 and 1.0 nM) and increasing concentrations of MB to characterize the equilibrium binding characteristics of MB at all subtypes (Fig. 3; for hM_2, hM_3, additional data are given in Online Resource 1, Fig. S3 for hM_1, hM_4, hM_5). MB concentration dependently inhibited specific radioligand binding at hM_2 and hM_3, the two subtypes which most markedly differed regarding the retarding effect of 100-μM MB on the [³H]NMS dissociation kinetics (Fig. 2). Not only at the low but also at the higher concentration of [³H]NMS, MB was able to decrease specific radioligand binding to levels not significantly different from bottom = 0% of specific control binding in the absence of MB. According to common knowledge (Christopoulos and Kenakin 2002), this finding makes ternary complex formation by MB (with the receptor and NMS) up to 1 μM rather unlikely (cf. Fig. 3a, b). Nevertheless, to make allowance for an allosteric action and to treat the data of all subtypes equal, we firstly analyzed the corresponding data for every subtype globally by means of an allosteric ternary complex model to obtain the measure of affinity K_X for MB binding to the respective orthosterically unliganded hM receptor subtype and cooperativity factors α quantifying a tentative ternary complex formation (consisting of MB/NMS/hM-receptor subtype, respectively). Very low α values not different from $\alpha = 0$ at all hM-receptor subtypes suggested a very

Fig. 2 Time course of dissociation of specific [^{3}H]NMS binding (1 nM) from the indicated M receptors (**a**–**e**) under control conditions (open circles) and in the presence of the 100-μM MB (filled circles). Dissociation was measured in control experiments after adding 1 μM of atropine alone, or, to check for an effect of MB, after adding MB together with atropine. Monoexponential curve fitting (cf. "Methods"). **f** Rate constant k_{-1} of [^{3}H]NMS dissociation in the presence of 100-μM MB as a percentage of the respective control value. The final concentrations of protein in the assay amounted to 10–40 μg/ml. Shown are representative experiments (**a**–**e**) carried out as duplicate determiniations and mean values ± S.E.M. (**f**) of three to four independent experiments
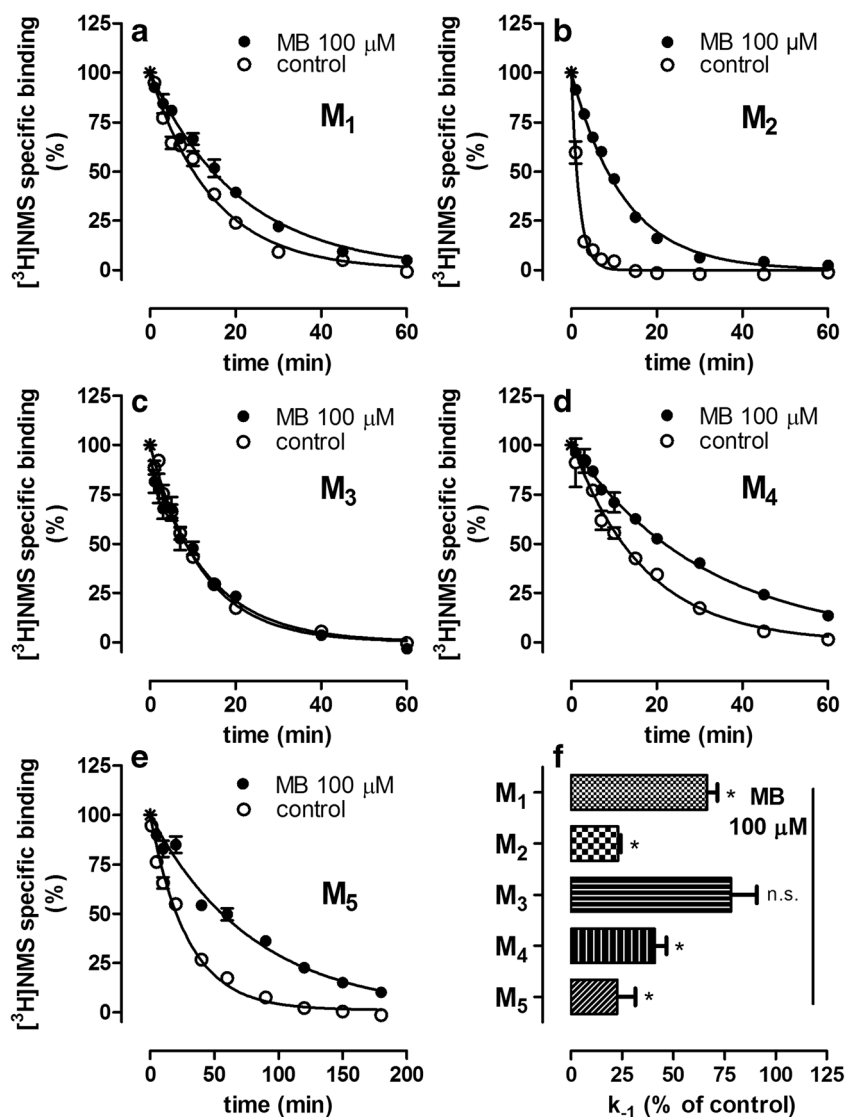
strong negative cooperativity between MB and NMS within a tentative ternary complex (Table 2). Accordingly, we analyzed these same heterologous inhibition data by means of a model assuming competition between MB and NMS at a single-receptor binding site (Fig. 3c, d). These global analyses yielded estimates for the binding affinity, expressed as K_i, of MB binding according to Cheng and Prusoff (1973) at the respective hM receptor subtypes (Table 2). Sharing the analysis parameter K_i for both curves instead of fitting individual K_i values for every curve revealed that increasing the concentration of [^{3}H]NMS from 0.2 to 1 nM (equivalent to a shift of NMS receptor occupancy from about 0.1 to 0.5, respectively) did *not* change significantly the resulting K_i of MB (cf. "Methods" for details). This finding is compatible with a formally competitive receptor interaction of NMS with sub-saturating concentrations of MB throughout all subtypes (*F* test, $P > 0.05$).

Competitive single-site binding inhibition analysis with Cheng-Prusoff correction at one low concentration of radioligand

In order to finally determine the K_i values for MB binding to all five hM receptor subtypes with great accuracy, the equilibrium inhibition data obtained with MB in the presence of 0.2-nM [^{3}H]NMS were chosen because they provided the lowest radioligand receptor occupancy (Fig. 4).

The respective parameters characterizing competitive MB binding at a single hM receptor binding site are listed in Table 3.

The affinity measures obtained were logK_i: hM$_3$ = 8.71 ± 0.15, n = 7, hM$_1$ = 8.68 ± 0.14, n = 6, hM$_5$ = 8.58 ± 0.07, n = 6, hM$_2$ = 8.27 ± 0,07, n = 6, hM$_4$ = 8.25 ± 0.11, n = 7. Statistically different was merely log$K_i$$hM_3$ from that found at hM$_4$ receptors (one-way ANOVA with Tukey's post-test, $P < 0.05$). In other words, the largest difference in binding

Table 1 Parameters characterizing the dissociation of $[^3\mathrm{H}]$NMS from the indicated muscarinic acetylcholine receptors in membranes of CHO cells in the absence and presence of 100-μM MB (cf. "Methods")

	hM1			hM2			hM3			hM4			hM5		
	Control	MB	n	Control	MB	n	Control	MB	n	Control	MB	n	Control	MB	n
k_{-1} (min^{-1})	0.073 ± 0.013	0.048 ± 0.008	4	0.490 ± 0.020	0.106 ± 0.005	4	0.078 ± 0.005	0.060 ± 0.005	3	0.042 ± 0.004	0.018 ± 0.005	3	0.032 ± 0.002	0.012 ± 0.002	5
$t_{1/2}$ (min)	10.7 ± 1.8	16.0 ± 2.4	4	1.4 ± 0.1	6.5 ± 0.3	4	8.9 ± 0.6	11.8 ± 1.2	3	17.5 ± 1.8	46.4 ± 8.1	3	23.0 ± 1.9	63.5 ± 10.0	5
Fold retardation	1.5			4.6			1.3			2.6			2.7		

Values are taken from analyses of the data shown in Fig. 3. k_{-1}: rate constant of $[^3\mathrm{H}]$NMS dissociation. $t_{1/2}$: half-life of $[^3\mathrm{H}]$NMS dissociation from the indicated M receptor subtypes. Fold retardation: retardation of $[^3\mathrm{H}]$NMS dissociation by 100-μM MB expressed as multiples of $t_{1/2,\text{control}}$ $[^3\mathrm{H}]$NMS dissociation. Given are mean values ± S.E.M. of three to four experiments carried out as quadruplicate determinations
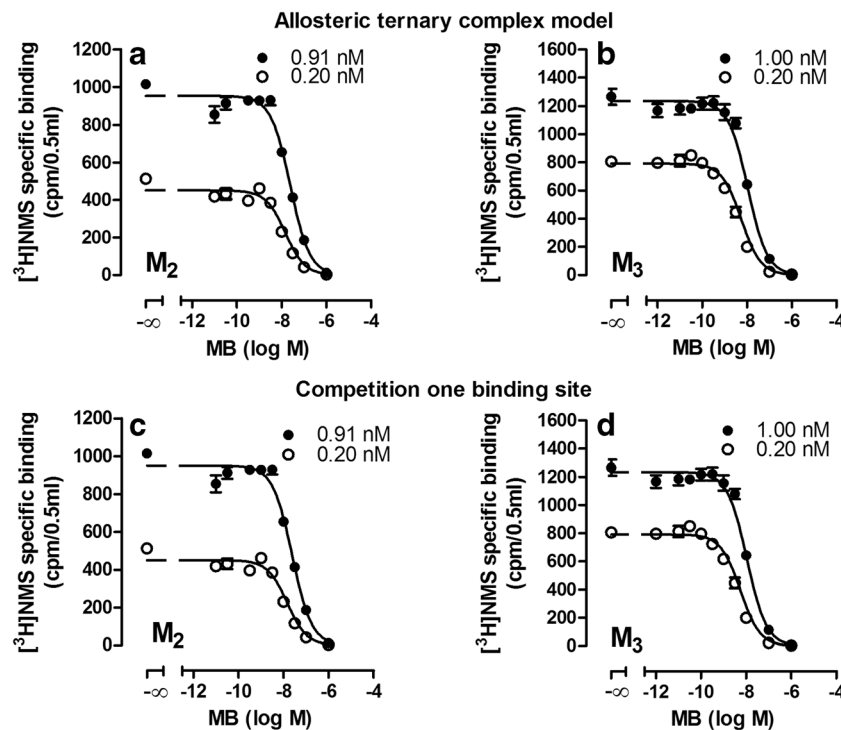
Fig. 3 Effect of MB on the equilibrium binding of the radioligand [^{3}H]NMS (0.2 and 1.0 nM) in membranes of CHO cells containing the indicated muscarinic acetylcholine receptors. Ordinate: specific [^{3}H]NMS binding cpm (count per minute) per 0.5-ml assay volume. Abscissa: log concentration of MB. Curves shown in A and B were obtained by nonlinear regression analysis applying Eq. (4) representing the ternary complex model of allosteric interactions to estimate the binding affinity constant K_X of MB at orthosterically unoccupied M receptors and its cooperativity α with NMS (cf. "Methods" and Table 3). Note that the lower plateau of the curves in **a** and **b** even at the higher concentration of radioligand did not differ from zero % specific

[^{3}H]NMS binding pointing against an allosteric interaction between NMS and MB (F test, $P > 0.05$). Additionally, K_I did not differ between the curves when treated as a non-shared versus a shared variable assuming a competitive interaction between NMS and MB at a single-receptor site (Eq. (5)) (**c**, **d**) (F test, $P > 0.05$). Incubations were carried out in HEPES buffer at 30 °C for 4 h at hM$_5$ receptors and for 2 h at the remaining subtypes (cf. Online Resource 1, Fig. S3). The final concentrations of membrane protein per assay volume amounted to 10–20 µg/ml for hM$_2$ and hM$_3$. Given are representative experiments carried out as quadruplicate determinations

constants amounted to log 0.46 which is equivalent to a factor of 2.9. Bearing in mind that a threefold difference can easily occur as a result of differences in biological susceptibility and

a methodological scatter (e.g., pipetting error) in the assay, the differences in binding constants K_i suggest MB to be a non-selective muscarinic receptor ligand.

Table 2 Parameters characterizing the binding of MB to membranes of CHO cells containing the indicated muscarinic acetylcholine receptors applying the allosteric ternary complex model (Tränkle et al. 2003) or assuming a competitive interaction with NMS at a single site (Tränkle et al. 2005) (cf. "Methods")

Model	Parameter	hM$_2$		hM$_3$	
		Mean	n	Mean	n
Allosteric ternary complex model (global fit)	logK_X MB	8.14 ± 0.06	6	8.61 ± 0.15	7
	α	0.011 ± 0.019	6	0.008 ± 0.016	7
One binding site (global fit)	logK_I MB	8.21 ± 0.06	6	8.66 ± 0.18	7
	logL_{low} [^{3}H]NMS	-9.70 ± 0.01	6	-9.71 ± 0.01	7
	logL_{high} [^{3}H]NMS	-9.02 ± 0.01		-9.01 ± 0.01	

logK_X: log affinity constant of MB binding to the respective orthosterically unlabeled M receptor subtype. α: factor of cooperativity between MB and NMS in ternary complexes such as MB/NMS/hM-receptor subtype with $\alpha < 1$, $\alpha > 1$, and $\alpha = 1$ suggesting negative, positive and neutral cooperativity, respectively. At every hM subtype, α was *not* different from $\alpha = 0$ (t test, $P > 0.05$). logK_I: equilibrium binding affinity constant of MB binding to the indicated orthosterically unlabeled M receptors. logL_{low} and logL_{high}: log concentrations of [^{3}H]NMS. Given are mean values ± S.E.M. of six to seven experiments carried out as quadruplicate determinations

Fig. 4 Effect of MB on the equilibrium binding of the radioligand [³H]NMS (at 0.2 nM, i.e., < 0.2 receptor occupancy) in membranes of CHO cells containing the indicated muscarinic acetylcholine receptors. Ordinate: specific [³H]NMS binding cpm (count per minute) per 0.5-ml assay volume. Abscissa: log concentration of MB. Curves were obtained by nonlinear regression analysis applying Eq. (5) (cf "Methods," "Data analysis") representing competition between MB and NMS at a single site of the receptor to measure the binding constant K_i of [³H]NMS binding inhibition by MB (cf. "Methods" and Table 3). Note that the low concentration of [³H]NMS applied means zone A of radioligand binding and assures measurement of true equilibrium binding constants K_i (Bennett and Yamamura 1985). Incubations were carried out in HEPES buffer (P1) at 30 °C for 4 h at hM$_5$ receptors and for 2 h at the remaining subtypes. The final concentrations of protein per assay volume amounted to 40 μg/ml for M$_5$ and 10–20 μg/ml for the remaining four subtypes. Given are representative experiments (**a**–**e**) carried out as quadruplicate determinations
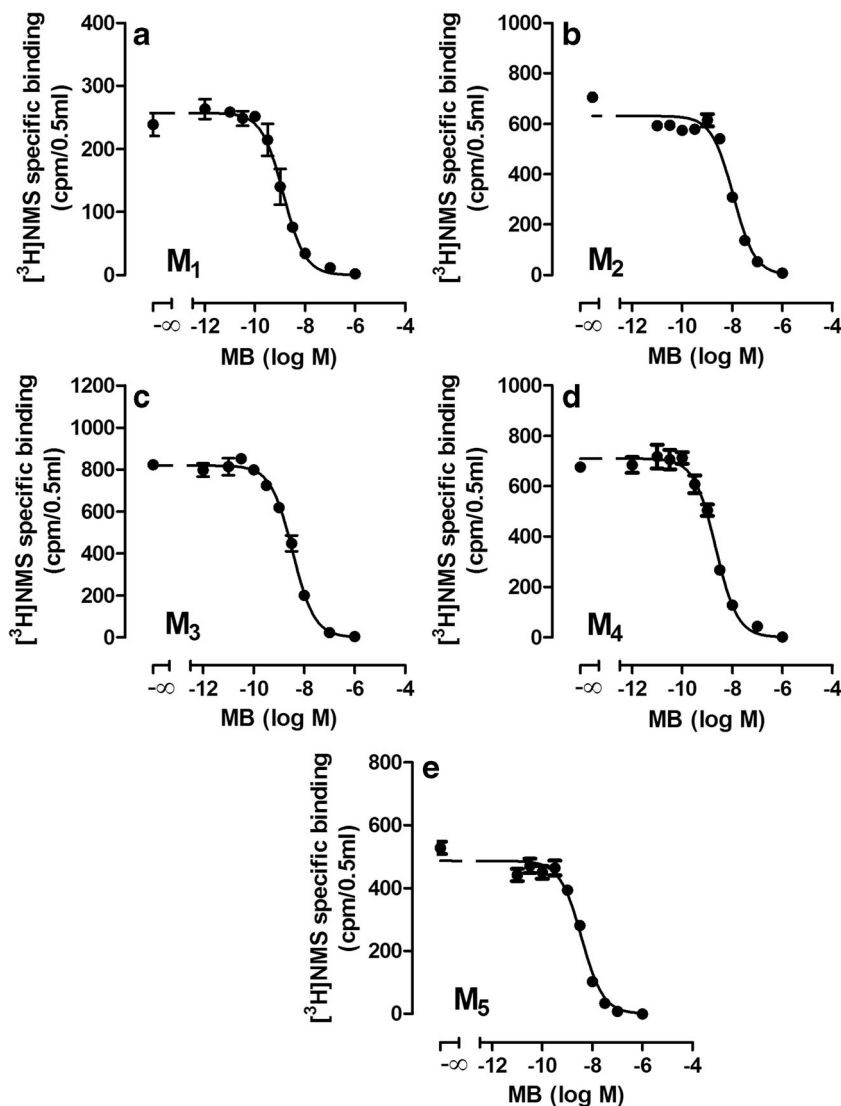
Functional properties of methanthelinium bromide

To extend the characterization to the level of receptor function, we studied the effect of MB on hM receptor signaling in hM$_1$–hM$_5$ receptors. In these experiments, we were able to determine the equilibrium affinity constant K_X and the corresponding cooperativity factor β for a tentative allosteric interaction and the equilibrium affinity constant K_B and the Schild slope s for a competitive interaction, respectively. In case of the hM$_1$-, hM$_3$-, and hM$_5$-subtypes, which couple preferably via $G_{q/11}$, we chose IP$_1$ accumulation as the readout to characterize the action of MB on ACh induced receptor stimulation. Furthermore, with hM$_2$-and hM$_4$- receptors, we used [³⁵S]GTPγS binding experiments to estimate the equilibrium

Table 3 Binding parameters obtained by fits to the data shown in Fig. 4

One binding site (single curves)	hM$_1$		hM$_2$		hM$_3$		hM$_4$		hM$_5$	
	Mean	n	Mean	n	Mean	n	Mean	n	Mean	n
logK_i MB	8.68 ± 0.14	6	8.27 ± 0.07	6	8.71 ± 0.15	7	8.25 ± 0.11	7	8.58 ± 0.07	6
logL_{low} [³H]NMS	-9.72 ± 0.01	6	-9.70 ± 0.004	6	-9.71 ± 0.01	7	-9.70 ± 0.004	7	-9.69 ± 0.004	6

The applied model assumes a competitive interaction of MB and NMS at a single binding site (cf. Methods). Measured data points were redrawn from Fig. 3. logK_i: log affinity binding constant of MB at the indicated orthosterically unlabeled M receptors. logL_{low}: log concentration of [³H]NMS (0.2 nM). Given are mean values ± S.E.M. of six to seven experiments carried out as quadruplicate determinations

affinity constant K_B of MB and its predominant type of receptor interaction via the Schild slope s. The concentration-effect curves in the absence and presence of increasing concentrations of MB at hM_2 and hM_3 receptors are illustrated in Fig. 5 (for the corresponding data and analyses at hM_1, hM_4, and hM_5 receptors cf. Online Resource 1, Fig. S4, and Table S4). Every ACh-induced control curve showed a slope not different from unity (F test, $P > 0.05$). In order to find out which model provided the best description for the action of MB, we, firstly, applied a ternary complex model and compared those findings, secondly, to a fit which assumed competition of MB and ACh at a single site (cf. "Methods"). The results obtained with hM_2 and hM_3 receptor data and the allosteric analyses yielded a measure of the equilibrium binding affinity K_X and the cooperativity factor β for the tentative interaction of MB with acetylcholine in MB/ACh/hM receptor complexes (Fig. 5). The corresponding β
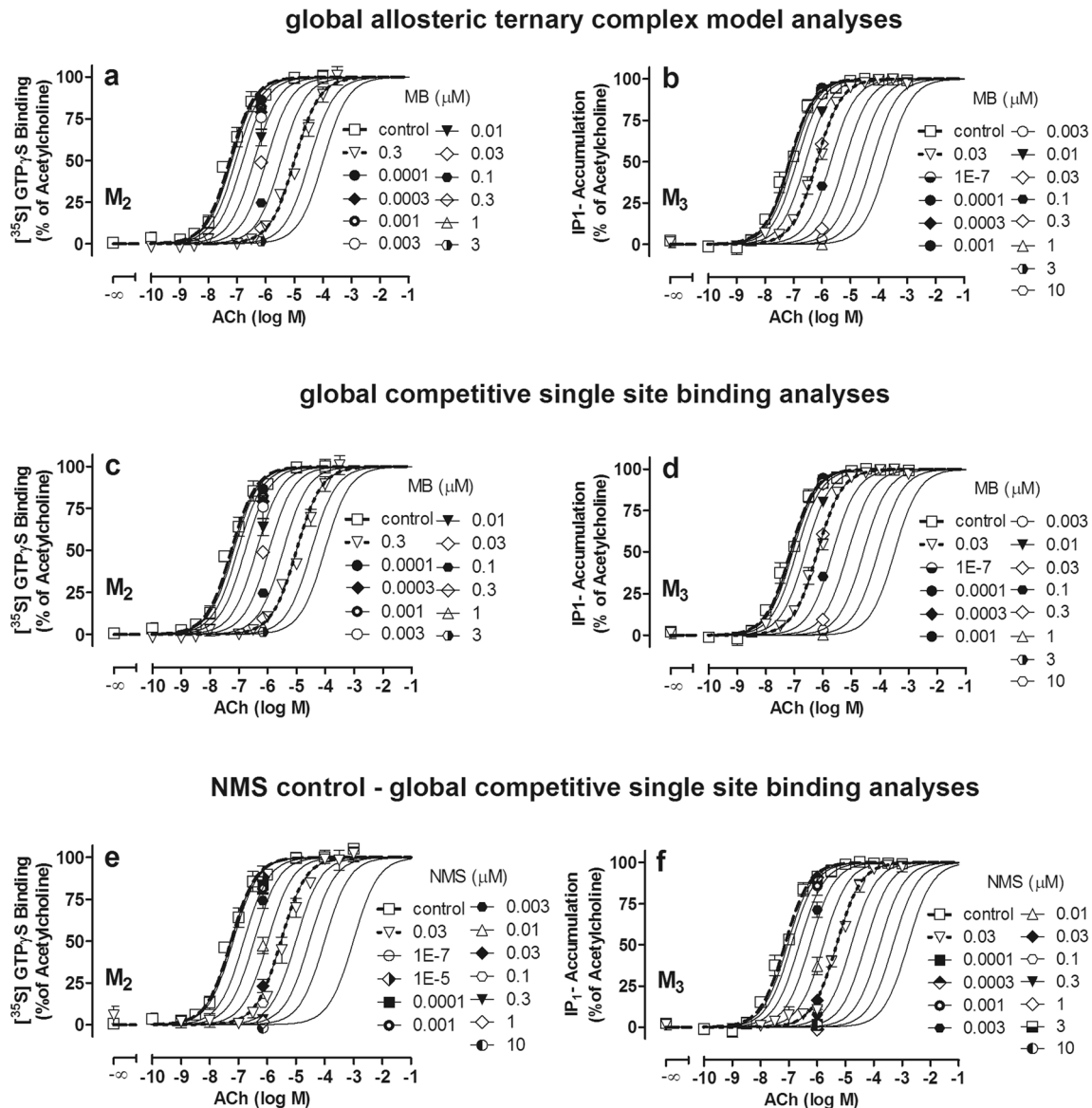
Fig. 5 a, c, and e Stimulation by ACh of [^{35}S]GTPγS (0.7 nM) binding to CHO membranes containing hM_2 in the presence of 1 μM GDP and several concentrations of MB (a–d) and NMS (e–f). Ordinate in a, c, and e: Binding of [^{35}S]GTPγS as a percentage of maximally induced binding. Abscissa: log concentration of ACh. Incubation were carried out in HEPES buffer at 30 °C for 1 h. b, d, and f Responses of intact living CHO cells expressing the indicated receptor hM receptor subtypes to ACh in IP$_1$ accumulation experiments. Ordinate: Accumulation of IP$_1$ as a percentage of the maximally induced response. Abscissa: log concentration of ACh. For each hM receptor, a control curve with variable concentrations of ACh only, a second set with increasing concentrations of MB, in the presence of one fixed ACh concentration (80–90% of the maximum receptor response induced by ACh) and, thirdly, an ACh curve shifted by a fixed concentration of MB or NMS, respectively, were conducted. a and b display a global nonlinear regression fit of the allosteric ternary complex model, whereas the fits in c, d, e, and f assume a competition at a single site. e and f demonstrate the corresponding results for the antagonist NMS as a control. The data points show the means and standard errors of at least quadruplicate observations

Table 4 Comparison of parameter values based on either an allosteric or a competitive model applied to data in Fig. 5 describing the effect of MB and NMS, respectively, on ACh induced effects in $[^{35}S]GTP\gamma S$ binding experiments at hM_2 and in IP_1 accumulation experiments at hM_3 receptors

Allosteric ternary complex model	M_2		M_3	
	Mean	n	Mean	n
$\log K_x$ MB	8.78 ± 0.07	8	8.43 ± 0.04	4
β MB	1.463e−16 ± 0.001037	8	3.7e−16 ± 0.001435	4
Competitive single-site model				
$\log K_B$ MB	8.79* ± 0.06	8	8.43* ± 0.04	4
s	0.98 ± 0.06	8	1.09 ± 0.09	4
$\log K_B$ NMS	9.25* ± 0.06	8	9.43* ± 0.04	4
s	1.24 ± 0.12	8	1.15 ± 0.08	4

$\log K_x$ describes the log affinity constant of MB binding to orthosterically unoccupied receptors; $\beta < 1$, $\beta > 1$, and $\beta = 1$ suggest negative, positive, and neutral cooperativity, respectively (Lazareno and Birdsall 1995; Tränkle et al. 2005). $\log K_B$ estimates the equilibrium log affinity constant of MB (and NMS) binding to the indicated receptors according to the competitive model (Waud 1975; Tränkle et al. 2005), s is the Schild slope. $\log L_{low}$ and $\log L_{high}$ are log concentrations of $[^3H]NMS$. $\log K_B$ values of MB are presented in comparison to NMS as a control. s was at no subtype statistically different from unity (F test) suggesting that MB and NMS acted competitively with ACh. Data are mean values of four to eight determinations performed as triple determinations. For more details see "Methods"

*$\log K_B$ values were determined with s constrained to unity, if s was not statistically different from $s = 1$ (F test, $P > 0.05$)

values were not different from zero throughout all subtypes (Table 4, t test, $P > 0.05$). This suggested a very strong negative cooperativity and is, at $\beta = 0$, identical to a competitive interaction between MB and ACh at all hM receptor subtypes.

Therefore, to finally determine the K_B values for MB, a model assuming competition with ACh at a single site was applied. While analyzing the corresponding data, firstly, the Schild slope factor s was estimated by global curve fitting. Since this value for the interaction between ACh and MB never differed from unity at any hM receptor subtype studied (F test, $P > 0.05$), $\log K_B$ values were determined with s constraint to unity. The results of the analyses shown in Fig. 5 are collected in Table 4. Further experiments applying the classical orthosteric competitive muscarinic antagonist NMS as standard served as a control and a check for our analyses with MB. The estimates of K_B for NMS in the current study were similar to values previously reported by Dei et al. in 2007 for native tissues. We had to compare our affinity measures with those findings from the latter group due to a lack of data in the literature on affinities collected in CHO cell membranes or living intact CHO cells.

The corresponding Schild slope factors s are in agreement with a competitive interaction as the best description for MB and NMS, respectively, with ACh, at all five hM subtypes (cf. Fig. 5, Table 4 and Fig. S4, Fig. S5, and Table S4).

Discussion

In the present study, we investigated whether and if, how MB, a drug widely used in conditions of hyperhidrosis axillaris (Cruddas and Baker 2017; Hund et al. 2004; Fuchslocher and Rzany 2002), binds to human M_1–M_5 muscarinic acetylcholine receptors in membranes from Chinese hamster ovary cells (hM_1–hM_5 CHO cells). Additionally, we looked at the MB effect on ACh mediated hM receptor function by measuring $G_{q/11}$ ($hM_1hM_3hM_5$) and $G_{i/o}$ (hM_2, hM_4) protein-mediated signaling. The study concentrated on muscarinic receptors because sweat production and the major route of sweat secretion are induced by cholinergic impulses (Cui and Schlessinger 2015, Sato et al. 1991). The experiments were carried out in comparison to the classical muscarinic antagonist N-methylscopolamine (NMS), either non-labeled in functional or as tritiated NMS ($[^3H]NMS$) in radioligand binding experiments. The hypothesis was that MB acts as a selective orthosteric competitive antagonist at hM_3 receptors, since eccrine sweat glands are activated predominantly through this muscarinic subtype (Schiavone and Brambilla 1991, Torres et al. 1991).

Firstly, we characterized $[^3H]NMS$ binding to hM receptors by homologous competition which provided estimates of the equilibrium affinity constant $K_{L,eq}$ in line with the literature, e.g., Wang and El-Fakahany 1993 (Fig. S1 and Table S1). Secondly, to check the validity of these $K_{L,eq}$ values the time course of $[^3H]NMS$ association to hM_1–hM_5 was determined to calculate the kinetic $K_{L,kin} = k_{+1}/k_{-1}$ (Table S2). Such a correspondence of the $K_{L,kin}$ values obtained at all five subtypes with their respective $K_{L,eq}$ values (Table S1) validates a radioligand binding assay (Limbird 1996) and thus the binding measurements applied in the current study.

Next, we looked for a tentative allosteric interaction of MB and NMS at the hM receptor subtypes by checking for any compound-induced allosteric change of $[^3H]NMS$ dissociation (Fig. 2). Compared to the control half-life, 100-μM MB delayed $[^3H]NMS$ dissociation and indicated the formation of ternary complexes (consisting of MB/NMS/hM-receptor, respectively) at this high concentration of MB in every hM subtype except for hM_3 (Fig. 2, Table 1) ranging from 1.5-fold at hM_1 to 4.6-fold at hM_2 compared to the respective control half-lives of $[^3H]NMS$. However, 100-μM MB is a concentration higher than necessary for a saturative occupation of the orthosteric/neurotransmitter binding site (expected at 100–$1000 \times K_L$ of a ligand) of the respective hM receptor subtype (see below). On the other hand is the absence of an allosteric effect of MB on the dissociation of $[^3H]NMS$ in hM_3 receptors not an obligatory hint to a

competition of MB with NMS at the orthosteric/neurotransmitter binding site. The atypical allosteric modulator of muscarinic receptors WIN 62,577 (17-beta-hydroxy-17-alpha-ethynyl-delta(4)-androstano[3,2-b]pyrimido[1,2-a]benzimidazole) can act allosterically on equilibrium orthosteric binding and action but lacks an effect on $[^3H]$Orthoster dissociation; it is an allosteric enhancer of ACh affinity at but does not affect $[^3H]$NMS dissociation from hM$_3$ receptors (Lazareno et al. 2002). However, a change of the rate of orthosteric radioligand dissociation is clearly indicative for the binding of a compound to a site different from the orthosteric/neurotransmitter receptor binding site (cf., e.g., De Amici et al. 2010 for review). In this respect, it should be noted that the conventional non-selective competitive muscarinic antagonist atropine can induce a—merely—twofold retardation of $[^3H]$NMS dissociation from porcine cardiac M$_2$ receptors in a buffer of very low ionic strength (5-mM "NaKPi buffer," Tränkle et al. 1996). Given the markedly higher ionic strength buffer applied in the binding experiments of the current study (i.e., 10-mM HEPES, 10-mM MgCl$_2$, and 100-mM NaCl, cf. "Methods"), the statistically significant 4.6-fold retardation of $[^3H]$NMS dissociation observed with MB at hM$_2$ in the current study is quite remarkable and prompted us not to restrict the analyses of MB interactions with the hM receptor subtypes to a competitive but to extend them to an allosteric perspective.

Heterologous inhibition experiments at 0.2 and 1 nM of $[^3H]$NMS served to characterize the equilibrium binding characteristics of MB to hM$_1$–hM$_5$ receptors. The formation of a bottom binding plateau of the inhibition curve above 0 % specific radioligand binding especially at the higher $[^3H]$NMS concentration could not be detected (as illustrated for the most and least sensitive hM$_2$ and hM$_3$ receptor in Fig. 3 and for all remaining subtypes in Fig. S3, Table S3). Such a behavior would have demasked an MB action at an allosteric site different from the orthosteric/neurotransmitter receptor site binding the radioligand (Lazareno and Birdsall 1995; Ehlert 1988). In contrast, MB was always able to inhibit specific radioligand binding at all hM-subtypes to 0% of control binding in the absence of MB (Fig. 3, Table 2 and Fig. S3, Table S3). This finding points against ternary complex formation by simultaneous binding of MB and NMS to the respective hM receptor subtype. In line with this, the analysis by the allosteric ternary complex model to obtain cooperativity factors β quantifying ternary complex formation, yielded β values not different from zero indicative of strong negative cooperativity (Fig. 3, Table 2 and Fig. S3, Table S3). Consequently, we analyzed these heterologous equilibrium inhibition binding data by means of a model assuming competition between MB and NMS at a single site (Fig. 3, Table 2 and Fig. S3, Table S3). This yielded estimates for the equilibrium affinity constant K_i of MB binding according to Cheng and Prusoff (1973) at the respective hM receptor subtype. Global data analyses applying parameter sharing (cf. "Methods") revealed that a fivefold increase of $[^3H]$NMS receptor occupancy did

not change the resulting K_i of MB (Fig. 3, Table 2 and Fig. S3, Table S3) which suggested a competitive binding interaction of NMS with sub-saturating concentrations of MB regarding receptor occupancy throughout all subtypes. Finally, we determined the affinity constants K_i of MB in hM receptors by heterologous inhibition at a low radioligand occupancy as illustrated in Fig. 4, Table 3. The values amounted to logK_i: hM$_3$: 8.71 ± 0.15, n = 7; hM$_1$: 8.68 ± 0.14, n = 6; hM$_5$: 8.58 ± 0.07, n = 6; hM$_2$: 8.27 ± 0.07, n = 6; hM$_4$: 8.25 ± 0.11, n = 7. However, though one statistical individual difference between the K_i values obtained at hM$_3$ and hM$_4$ receptors (one-way ANOVA with Tukey's post-test, P < 0.05) was observed (Fig. 6a), the relevance of this threefold subtype selectivity of MB binding may be doubted.

Whereas the most direct means for detecting and quantifying allosteric interactions at GPCRs are binding assays, functional approaches to receptor action can also be used (Christopoulos and Kenakin 2002). The earliest evidence of receptor allosterism relied on these types of experiments (Lüllmann et al. 1969) and was later proven in radioligand binding experiments (Jepsen et al. 1988). Therefore, in addition to the experiments characterizing the binding of MB, we carried out functional experiments to access the effect of MB in comparison to the conventional
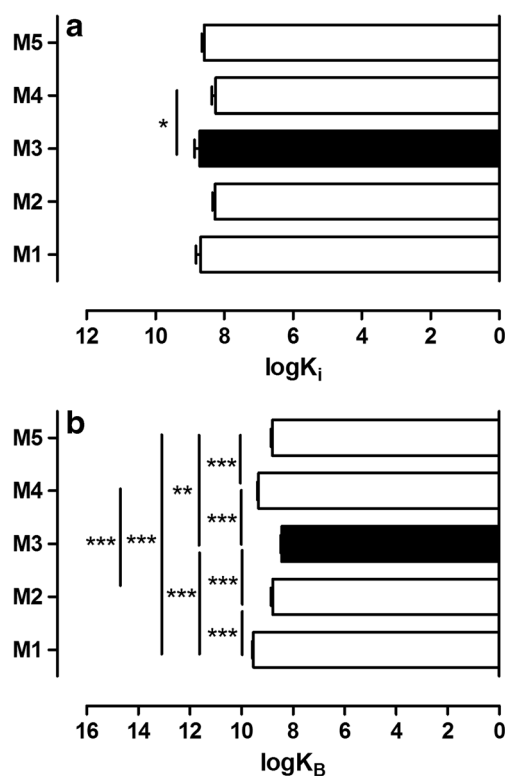
Fig. 6 Binding constants of MB at the indicated hM acetylcholine receptor subtypes obtained in binding and functional experiments. **a** logK_i: (log) equilibrium affinity inhibition binding constant. **b** logK_B: (log) equilibrium affinity constant determined in functional experiments. Asterisk symbols: Statistical differences detected by one-way ANOVA with Tukey's post-test, *, $P < 0.05$, **, $P < 0.001$, *** $P < 0.0001$). For further details see text

antagonist NMS on hM-receptor mediated function. We measured agonist mediated receptor activation via G-proteins mediating the respective signaling pathway preferred by ACh in the respective hM subtypes (e.g., Wess et al. 2007). ACh was chosen as an agonist because the CHO cells applied lack AChE (Lazareno and Birdsall 1995). Regarding the non-enzymatic hydrolytic stability of ACh solutions at 25 °C, ACh is stable over a period of 28 days (Sletten et al. 2005). Thus, ACh concentrations can be considered constant during the duration of the experiments of the current study. Finally, the endogenous ACh plays the most important role in muscarinic receptor activation in glandular tissue (Grant et al. 1995). Since the effect of an allosteric agent may depend on the structure of the orthosteric ligand, i.e., may be different for ACh compared with NMS used in the binding experiments (e.g., Lazareno and Birdsall 1995), we, in the functional experiments, followed the strategy applied in the binding experiments (see above) and, firstly, checked for an allosteric effect of MB on the action of ACh with the simple ternary complex model (Fig. 5a–b, Table 4 and Fig. S4a, c, e, and Table S4). According to this model (Lazareno and Birdsall 1995), an allosteric agent will alter orthosteric ligand affinity but not its efficacy. It will shift the concentration-response curves of an orthosteric agonist without changing the basal and maximal cell response or the curve shape and slope in a parallel fashion. In the case of a positive or a negative cooperativity, the agonist curves would be displaced to the left or to the right, respectively (Christopoulos and Kenakin 2002). A check of a parallel curve shift of the ACh control curve by MB documenting unchanged upper and lower plateaux (see above) is representatively shown for hM$_2$ and hM$_3$ receptors in Fig. S6. We found the cooperativity factor β as a measure for the extent and direction of a tentative effect within an allosteric ternary complex (consisting of MB/ACh/hM-receptor) to be not different from $\beta = 0$ at all hM-receptor subtypes (one-sample t test, $P > 0.05$). This suggested a strong negative cooperativity of MB with ACh. A competitive interaction can be distinguished from a strong negative allosteric cooperativity if the effects of as large a range of antagonist concentrations as is practicable is studied (Christopoulos and Kenakin 2002). As can be seen from Fig. 5a, b, Table 4 and Fig. S4a, c, e, and Table S4, this was accomplished in the current study by applying MB up to saturating concentrations equivalent to 300–1000-fold of its respective K_i value at the individual subtypes (cf. Table 3). Therefore, we concluded a competitive interaction at sub-saturating concentrations of MB and fitted the functional data for every hM subtype to a model assuming competition of MB and ACh at a single-receptor site, according to Lazareno and Birdsall (1993). This model is a modified version of the Schild method (Arunlakshana and Schild 1959) with the aim to reduce the number of data points needed to fit the model and was carried out here according to Tränkle et al. (2005). In addition to K_B as a functional binding constant, this model gives the Schild slope factor s, a parameter suitable to discriminate a competitive from

a non-competitive interaction between two receptor ligands. In every case, our calculations for MB and for the well-known orthosteric antagonist NMS yielded no difference in s from unity, which is in line with a competitive interaction of MB and NMS, respectively, with ACh (Fig. 5c–f, Table 4 and Fig. S4b, d, f, and Table S4). The affinity constants amounted to: logK_B: hM$_1$: 9.53 ± 0.04, $n = 8$; hM$_4$: 9.33 ± 0.05, $n = 5$; hM$_5$: 8.80 ± 0.05, $n = 5$; hM$_2$: 8.79 ± 0.06, $n = 8$; hM$_3$: 8.43 ± 0.04, $n = 4$. Thus, functionally, MB preferred to act 13-fold stronger at hM$_1$ and eightfold stronger at hM$_4$ receptors compared to hM$_3$ receptors; the functional MB affinity at hM$_2$ was still twofold and significantly higher than at hM$_3$ receptors. A collection of individual statistical differences (one-way ANOVA with Tukey's post-test, $P < 0.05$) between logK_B obtained at the different subtypes is illustrated in Fig. 6b. It is known from the anticholinergic compound tolderodine, that shows, in vivo, in patients with overactive bladder syndrome, functional selectivity for hM$_3$ receptors but no binding selectivity in either hM$_1$–hM$_5$ receptors in CHO cells or between M$_3$ and M$_2$ receptors from urinary bladder and parotid gland, respectively, in native guinea pig tissues (Nilvebrant et al. 1997). Future studies will have to address whether in humans, MB acts in a similar fashion with functional selectivity for hM$_3$ receptors in eccrine sweat cells.

In summary, MB binds to and functions at all five hM receptor subtypes in the nanomolar concentration range. MB binding and function at hM$_3$ receptors occur in a formally competitive fashion at all concentrations studied. At the remaining hM subtypes, MB binding below 1 μM, and action below 10 μM is competitive, whereas MB tends to act allosterically at 100 μM, the highest concentration applied in the current study. There was no evidence for a therapeutically exploitable degree of subtype-selectivity of MB binding or action among the five muscarinic receptor subtypes. MB can thus be considered to be a competitive non-selective orthosteric muscarinic receptor antagonist in CHO cells.

Compliance with ethical standards

The authors declare the current study to comply with ethical standards.

Conflict of interest Author CT received two research grants from RIEMSER Pharma GmbH. During the start of the study, the position of author MI was funded by the first of these grants.

References

Arunlakshana O, Schild HO (1959) Some quantitative uses of drug antagonists. Br J Pharmacol Chemother 14(1):48–58

Bennett JP, Yamamura HI (1985) Neurotransmitter, hormone, or drug receptor binding methods. In: Neurotransmitter receptor binding. Raven Press, New York, pp 61–89

Bock A, Chirinda B, Krebs F, Messerer R, Bätz J, Muth M, Dallanoce C, Klingenthal D, Tränkle C, Hoffmann C, De Amici M, Holzgrabe U, Kostenis E, Mohr K (2014) Dynamic ligand binding dictates partial agonism at a G protein-coupled receptor. Nat Chem Biol 10(1):18–20. https://doi.org/10.1038/nCHeMBIO.1384

Caulfield MP, Birdsall NJ (1998) International Union of Pharmacology. XVII. Classification of muscarinic acetylcholine receptors. Pharmacol Rev 50(2):279–290

Chen X, Klöckner J, Holze J, Zimmermann C, Seemann WK, Schrage R, Bock A, Mohr K, Tränkle C, Holzgrabe U, Decker M (2014) Rational design of partial agonists for the muscarinic m1 acetylcholine receptor. J Med Chem 58(2):560–576. https://doi.org/10.1021/jm500860w

Cheng YC, Prusoff WH (1973) Relationship between the inhibition constant (Ki) and the concentration of inhibitor which causes 50 per cent inhibition (I50) of an enzymatic reaction. Biochem Pharmacol 22(23):3099–3108. https://doi.org/10.1016/0006-2952(73)90196-2

Christopoulos A, Kenakin T (2002) G protein-coupled receptor allosterism and complexing. Pharmacol Rev 54(2):323–374

Clark AJ (1933) Mode of action of drugs on cells. Edward Arnold, London

Cruddas L, Baker DM (2017) Treatment of primary hyperhidrosis with oral anticholinergic medications: a systematic review. J Eur Acad Dermatol Venereol 31(6):952–963. https://doi.org/10.1111/jdv.14081

Cui CY, Schlessinger D (2015) Eccrine sweat gland development and sweat secretion. Exp Dermatol 24(9):644–650. https://doi.org/10.1111/exd.12773

De Amici M, Dallanoce C, Holzgrabe U, Tränkle C, Mohr K (2010) Allosteric ligands for G protein-coupled receptors: a novel strategy with attractive therapeutic opportunities. Med Res Rev 30(3):463–549. https://doi.org/10.1002/med.20166

DeBlasi A, O'Reilly K, Motulsky HJ (1989) Calculating receptor number from binding experiments using same compound as radioligand and competitor. Trends Pharmacol Sci 10(6):227–229. https://doi.org/10.1016/0165-6147(89)90266-6

Dei S, Bellucci C, Buccioni M, Ferraroni M, Guandalini L, Manetti D, Martini E, Marucci G, Matucci R, Nesi M, Romanelli MN, Scapecchi S, Teodori E (2007) Synthesis, affinity profile, and functional activity of muscarinic antagonists with a 1-Methyl-2-(2,2-alkylaryl-1,3-oxathiolan-5-yl)pyrrolidine Structure. J Med Chem 50(6):1409–1413

Ehlert FJ (1988) Estimation of the affinities of allosteric ligands using radioligand binding and pharmacological null methods. Mol Pharmacol 33(2):187–194

Fredriksson R, Lagerström MC, Lundin LG, Schiöth HB (2003) The G-protein-coupled receptors in the human genome form five main families. Phylogenetic analysis, paralogon groups, and fingerprints. Mol Pharmacol 63(6):1256–1272. https://doi.org/10.1124/mol.63.6.1256

Fuchslocher M, Rzany B (2002) Oral anticholinergic therapy of focal hyperhidrosis with methanthelinium bromide (Vagantin). Initial data on effectiveness. Hautarzt 53(2):151–152. https://doi.org/10.1007/s00105-001-0328-2

Grant MP, Francis NJ, Landis SC (1995) The role of acetylcholine in regulating secretory responsiveness in rat sweat glands. Mol Cell Neurosci 6(1):32–42. https://doi.org/10.1006/mcne.1995.1004

Haga K, Kruse AC, Asada H, Yurugi-Kobayashi T, Shiroishi M, Zhang C, Weis WI, Okada T, Kobilka BK, Haga T, Kobayashi T (2012) Structure of the human M2 muscarinic acetylcholine receptor bound to an antagonist. Nature 482(7386):547–551. https://doi.org/10.1038/nature10753. doi:10.1038/nature10753

Hall DA (2000) Modeling the functional effects of allosteric modulators at pharmacological receptors: an extension of the two-state model of receptor activation. Mol Pharmacol 58(6):1412–1423. https://doi.org/10.1124/mol.58.6.1412

Hexsel D, Camozzato FO (2018) Hyperhidrosis. In: Bonamigo RR, Dornelles SIT (eds) Dermatology in public health environments. Springer, Cham. https://doi.org/10.1007/978-3-319-33919-1_67

Hulme EC, Trevethick MA (2010) Ligand binding assays at equilibrium: validation and interpretation. Br J Pharmacol 161(6):1219–1237. https://doi.org/10.1111/j.1476-5381.2009.00604.x

Hulme EC, Birdsall NJM, Buckley NJ (1990) Muscarinic receptor subtypes. Annu Rev Pharmacol Toxicol 30(1):633–673

Hund M, Sinkgraven R, Rzany B (2004) Randomized, placebo-controlled, double blind clinical trial for the evaluation of the efficacy and safety of oral methantheliniumbromide (Vagantin) in the treatment of focal hyperhidrosis. J Dtsch Dermatol Ges 2(5):343–349

Jepsen K, Lüllmann H, Mohr K, Pfeffer J (1988) Allosteric stabilization of 3H-N-methylscopolamine binding in guinea-pig myocardium by an antidote against organophosphate intoxication. Basic Clin Pharmacol Toxicol 63(3):163–168. https://doi.org/10.1111/j.1600-0773.1988.tb00932.x

Kruse AC, Hu J, Kobilka BK, Wess J (2014a) Muscarinic acetylcholine receptor X-ray structures: potential implications for drug development. Curr Opin Pharmacol 16:24–30. https://doi.org/10.1016/j.coph.2014.02.006

Kruse AC, Kobilka BK, Gautam D, Sexton PM, Christopoulos A, Wess J (2014b) Muscarinic acetylcholine receptors: novel opportunities for drug development. Nat Rev Drug Discov 13(7):549–560. https://doi.org/10.1038/nrd4295

Lagerström MC, Schiöth HB (2008) Structural diversity of G protein-coupled receptors and significance for drug discovery. Nat Rev Drug Discov 7(4):339–357. https://doi.org/10.1038/nrd2518

Lazareno S, Birdsall NJM (1993) Pharmacological characterization of acetylcholine-stimulated [35S]-GTPγS binding mediated by human muscarinic m1–m4 receptors: antagonist studies. Br J Pharmacol 109(4):1120–1127. https://doi.org/10.1111/j.1476-5381.1993.tb13738.x

Lazareno S, Birdsall NJ (1995) Detection, quantitation, and verification of allosteric interactions of agents with labeled and unlabeled ligands at G protein-coupled receptors: interactions of strychnine and acetylcholine at muscarinic receptors. Mol Pharmacol 48(2):362–378

Lazareno S, Popham A, Birdsall NJM (2002) Analogs of WIN 62,577 define a second allosteric site on muscarinic receptors. Mol Pharmacol 62(6):1492–1505. https://doi.org/10.1124/mol.62.6.1492

Limbird LE (1996) Identification of receptors using direct radioligand binding techniques. In: Cell surface receptors: a short course on theory and methods. Springer, Boston, pp 61–122

Lüllmann H, Ohnesorge FK, Schauwecker GC, Wassermann O (1969) Inhibition of the actions of carbachol and DFP on guinea pig isolated atria by alkane-bis-ammonium compounds. Eur J Pharmacol 6(3):241–247. https://doi.org/10.1016/0014-2999(69)90181-2

Motulsky H, Christopoulos A (2004) Fitting models to biological data using linear and nonlinear regression: a practical guide to curve fitting. Oxford University Press, Oxford

Nilvebrant L, Hallén B, Larsson G (1997) Tolterodine—a new bladder selective muscarinic receptor antagonist: preclinical pharmacological and clinical data. Life Sci 60(13–14):1129–1136

Sato K, Ohtsuyama M, Samman G (1991) Eccrine sweat gland disorders. J Am Acad Dermatol 24(6):1010–1014

Schiavone A, Brambilla A (1991) Muscarinic M3 receptors mediate secretion from sweat glands in the rat. Pharmacol Res 23(3):233–239. https://doi.org/10.1016/S1043-6618(05)80082-9

Schmitz J, van der Mey D, Bermudez M, Klöckner J, Schrage R, Kostenis E, Tränkle C, Wolber G, Mohr K, Holzgrabe U (2014) Dualsteric muscarinic antagonists–orthosteric binding pose controls allosteric subtype selectivity. J Med Chem 57(15):6739–6750. https://doi.org/10.1021/jm500790x

Sletten DM, Nickander KK, Low PA (2005) Stability of acetylcholine chloride solution in autonomic testing. J Neurol Sci 234:1), 1–1), 3. https://doi.org/10.1016/j.jns.2005.02.007

Stockton JM, Birdsall NJ, Burgen AS, Hulme EC (1983) Modification of the binding properties of muscarinic receptors by gallamine. Mol Pharmacol 23(3):551–557

Torres NE, Zollman PJ, Low PA (1991) Characterization of muscarinic receptor subtype of rat eccrine sweat gland by autoradiography. Brain Res 550(1):129–132. https://doi.org/10.1016/0006-8993(91)90415-R

Tränkle C, Kostenis E, Burgmer U, Mohr K (1996) Search for lead structures to develop new allosteric modulators of muscarinic receptors. J Pharmacol Exp Ther 279(2):926-933

Tränkle C, Weyand O, Voigtländer U, Mynett A, Lazareno S, Birdsall NJ, Mohr K (2003) Interactions of orthosteric and allosteric ligands with [^{3}H] dimethyl-W84 at the common allosteric site of muscarinic M2 receptors. Mol Pharmacol 64(1):180–190. https://doi.org/10.1124/mol.64.1.180

Tränkle C, Dittmann A, Schulz U, Weyand O, Buller S, Jöhren K, Heller E, Birdsall NJM, Holzgrabe U, Ellis J, Höltje HD, Mohr K (2005) Atypical muscarinic allosteric modulation: cooperativity between modulators and their atypical binding topology in muscarinic M2 and M2/M5 chimeric receptors. Mol Pharmacol 68(6):1597–1610. https://doi.org/10.1124/mol.105.017707

Wang SZ, El-Fakahany EE (1993) Application of transfected cell lines in studies of functional receptor subtype selectivity of muscarinic agonists. J Pharmacol Exp Ther 266(1):237–243

Waud DR (1975) Analysis of dose—response curves. In: Daniel EE, Paton DM (eds) Smooth muscle. Springer, Boston. https://doi.org/10.1007/978-1-4684-2751-6_27

Wess J (2004) Muscarinic acetylcholine receptor knockout mice: novel phenotypes and clinical implications. Annu Rev Pharmacol Toxicol 44:423–450. https://doi.org/10.1146/annurev.pharmtox.44.101802.121622

Wess J, Eglen RM, Gautam D (2007) Muscarinic acetylcholine receptors: mutant mice provide new insights for drug development. Nat Rev Drug Discov 6(9):721–733. https://doi.org/10.1038/nrd2379

Williams, M. (1993), Receptor-ligand interactions. A practical approach. E.C. Hulme, ed. IRL Press/Oxford University Press, New York, 1992, xx + 458 pp, paperback. Drug Dev Res, 30: 54. https://doi.org/10.1002/ddr.430300108